Journal of Hazardous Materials 183 (2010) 35–43

Contents lists available at ScienceDirect

Journal of Hazardous Materials

journal homepage: www.elsevier.com/locate/jhazmat

Equilibrium, kinetic and thermodynamic studies on aluminum biosorption by a mycelial biomass (*Streptomyces rimosus*)

Amina Tassist*, Hakim Lounici, Nadia Abdi, Nabil Mameri

Laboratory of Environmental Biotechnologies and Process Engineering, BIOGEP, Polytechnic National School of Algiers, Hacen Badi, El Harrach, Algiers, Algeria

ARTICLE INFO

Article history:
Received 14 February 2010
Received in revised form 19 May 2010
Accepted 18 June 2010
Available online 26 June 2010

Keywords:
Aluminum
Biosorption
S. rimosus
Thermodynamics
Ion exchange

ABSTRACT

This work focused on kinetic, equilibrium and thermodynamic studies on aluminum biosorption by *Streptomyces rimosus* biomass. Infrared spectroscopy analysis shows that *S. rimosus* present some groups: hydroxyl, methyl, carboxyl, amine, thiol and phosphate. The maximum biosorption capacity of *S. rimosus* biomass was found to be 11.76 mg g^{-1} for the following optimum conditions: particle size,]250–560] μm, pH 4–4.25, biomass content of 25 g L^{-1}, agitation of 250 rpm and temperature of 25 °C. Langmuir, Freundlich and Dubinin–Radushkevich (D–R) models were applied to describe the biosorption isotherms at free pH (pH_i 4) and fixed pH (pH_f 4). Langmuir model is the most adequate. With fixed pH, the maximum biosorption capacity is enhanced from 6.62 mg g^{-1} to 11.76 mg g^{-1}. The thermodynamic parameters (ΔG°, ΔH° and ΔS°) showed the feasibility, endothermic and spontaneous nature of the biosorption at 10–80 °C. The activation energy (Ea) was determined as 52.18 kJ mol^{-1} using the Arrhenius equation and the rate constant of pseudo-second-order model (the most adequate kinetic model). The mean free energy was calculated as 12.91 kJ mol^{-1} using the D–R isotherm model. The mechanism of Al(III) biosorption on *S. rimosus* could be a chemical ion exchange and carboxyl groups are mainly involved in this mechanism.

1. Introduction

Aluminum is widely used in many industries; it is therefore massively rejected in the environment. It is used in the transformation industry (manufacturing of light alloy for aeronautic, automobile, domestic utensils, boats, packing, . . .) [1,2]. Aluminum is also used in the chemical industry as a catalyst, pigment, agent of skin tanning and tissue mordanting. It is involved in the composition of abrasives, ink, cement and explosives [1,3]. It is also used in the pharmaceutical industry, in anti diarrheic and antacid preparations [3].

Aluminum is a very reactive element. Its bonds are strong and difficult to displace [4]. It can accumulate in the cell leading to the formation of voluminous deposits incompatible with the good working process and the cellular life [5]. Therefore, aluminum is involved in the apparition of Alzheimer's disease among aged subjects exposed to a concentration greater than 110 μg L^{-1} in drinking water and also the cause of two severe neuro-degenerative diseases: amyotrophic lateral sclerosis and Parkinson [6,7].

In soft water, aluminum has a toxic action after a week of contact with a concentration of 0.1 mg L^{-1}. At higher dose of 88 mg L^{-1} of $AlCl_3$, it may cause death to some fish within a long action time. At 132 mg L^{-1} of $AlCl_3$, most of fish perish in a few hours. In plants, the toxic action of aluminum on germs of squash, corn, beans, rice and wheat was noticed in acid soils provoking a decrease of phosphoric acid absorption. In barley and millet, bad effects (as an intoxication of the roots) appear at a concentration of 1 mg L^{-1}. In aquatic plants, the presence of 0.005–0.01% of aluminum salt provokes a weakening and some assimilation troubles. Corn cultivated in an aqueous medium with increasing doses of aluminum from 10^{-10} mg L^{-1} to 100 mg L^{-1} was affected both in its growth and fruitfulness. The utmost of toxicity for *Scenedesmus* algae is about 1.5 mg L^{-1} and 136 mg L^{-1} for *Daphnia magna* [8].

The biosorption is currently considered as an alternative process for metallic pollutant elimination. It is simple, efficient and economic. In the case of aluminum, different types of adsorbents were used: starch, clay, activated charcoal, wood charcoal [9], date-pit and BDH activated carbon [10], plants [11], algae [12,13], mushrooms [14,15] and bacteria [16]. The present study proposes a new biosorbent for the treatment of waters charged with aluminum: *Streptomyces rimosus*, mycelial bacteria, Gram+, belonging to actinomycetes. This biomass constitutes a solid waste of

* Corresponding author. Tel.: +213 7 71 68 39 67; fax: +213 25 58 12 53.
E-mail address: aminatassist@yahoo.fr (A. Tassist).

0304-3894/$ – see front matter © 2010 Elsevier B.V. All rights reserved.
doi:10.1016/j.jhazmat.2010.06.078

SAIDAL pharmaceutical industry, unit of Medea (Algeria), support of oxytetracyclin production. This biosorbent proved its efficiency for the treatment of waters charged with heavy metals such as zinc [17–20], copper [19,20], chromium [19], lead [21], cadmium [22], nickel [20,23] and iron [24].

In this work the biosorption of aluminum on *S. rimosus* is investigated. The biosorbent structure is characterized by infrared spectroscopy and biosorption tests were carried out in batch mode. Several parameters were optimized: particle size, biosorbent content, agitation, temperature and pH. The equilibrium biosorption data were evaluated by Langmuir, Freundlich and Dubinin–Radushkevich (D–R) isotherm models at free pH (pH_i 4) and fixed (pH_f 4). Some thermodynamic parameters were also calculated in order to describe the biosorption mechanism of Al(III) on *S. rimosus* biomass.

2. Materials and methods

2.1. Biosorbent preparation

The biosorbent, *S. rimosus*, was provided by SAIDAL antibiotics unit of Medea (Algeria). The biomass wafers were cleaved, laid out on big trays and dried by air. When the biomass is dry, it is washed several times with distilled water then dried in air for 24 h and finally baked at 50 °C for another 24 h. The clean biomass is mechanically ground and sifted to get a powder of different particle sizes: ≤140 μm,]140–250] μm,]250–560] μm,]560–800] μm, by means of sifters (800 μm, 560 μm, 250 μm and 140 μm).

2.2. Structural characterization by infrared spectroscopy analysis

A sample of biomass is mixed with dry KBr in a ratio of 1 mg/300 mg. The mixture is ground and compressed. The obtained tablet is analyzed in a Perkin-Elmer spectrometer in the interval of 400–4000 cm^{-1}.

2.3. Aluminum biosorption kinetic

The kinetic curves describing the biosorption of Al(III) ions were determined by measuring the metallic ion concentrations at short and regular intervals. The samples were filtered by means of Wathman paper N°5 and analyzed by spectrophotometry technique using the *Palintest*® and *Lovibond* reactants. This technique is a standardized method for water analysis (ASTM). As the biosorption is a recommended process for the treatment of weak concentrations, initial concentration of 30 mg L^{-1} for optimization tests was used.

2.3.1. Effect of particle size

The contact surface between the solid phase of the biosorbent and the liquid phase plays an important role in the biosorption phenomena. The best particle size range is the one that presents a compromise between the biosorption quality and the mechanical behavior. Biosorption essays were achieved under the following conditions: an initial concentration C_0 = 30 mg L^{-1}, a solution volume of 250 mL, an initial pH: pH_i 3.98, a stirring speed ω = 250 rpm, a temperature T = 25 °C and a biosorbent content m = 20 g L^{-1} for various particle sizes: ≤140 μm,]140–250] μm,]250–560] μm,]560–800] μm.

2.3.2. Effect of biosorbent content

In order to optimize the biomass quantity requisite for a maximal fixation of metallic ions, the effect of the ratio: (biosorbent mass/solution volume) on the aluminum biosorption capacity was investigated. The particle size ranging from 250 μm to 560 μm, C_0 = 30 mg L^{-1}, the solution volume was 250 mL, pH_i 3.98, the stirring speed ω = 250 rpm, the temperature T = 25 °C and the biosorbent content varied from 5 g L^{-1} to 30 g L^{-1}.

2.3.3. Effect of agitation

In solid–liquid system, the role of the agitation is to homogenize the particles in the liquid phase and to increase the diffusion around the particles. Thus, it proves to be useful to determine the optimal agitation speed, we studied the biosorption kinetics of Al(III) for different agitation speeds (50–1000 rpm). The particle size ranging from 250 μm to 560 μm, the biosorbent content m = 25 g L^{-1}, C_0 = 30 mg L^{-1}, the solution volume was 250 mL, pH_i 3.98, the temperature T = 25 °C.

2.3.4. Effect of temperature (biosorption thermodynamics)

To study the effect of this parameter, the biosorption at temperatures of 10 °C, 25 °C, 50 °C and 80 °C was studied. The particle size ranging from 250 μm to 560 μm, the biosorbent content m = 25 g L^{-1}, the stirring speed ω = 250 rpm, C_0 = 30 mg L^{-1}, the solution volume was 250 mL, pH_i 3.98, the stirring speed ω = 250 rpm.

2.3.4.1. Evaluation of thermodynamic parameters (ΔG°, ΔH° and ΔS°). In order to describe the thermodynamic behavior of aluminum biosorption by *S. rimosus* biomass, thermodynamic parameters including the change in free energy (ΔG°), enthalpy (ΔH°) and entropy (ΔS°) were calculated from the following equation:

$$\Delta G^\circ = -RT \ln K_D \quad (1)$$

where R is the universal gas constant (8.314 J mol^{-1} K^{-1}), T is the temperature (K) and K_D (q_e/C_e) is the distribution coefficient [25–30]. The enthalpy (ΔH°) and entropy (ΔS°) parameters were estimated from the following equation:

$$\ln K_D = \frac{\Delta S^\circ}{R} - \frac{\Delta H^\circ}{RT} \quad (2)$$

2.3.4.2. Determination of activation energy. The activation energy Ea was determined using the Arrhenius equation [31,32]

$$\ln k = \ln A - \frac{Ea}{RT} \quad (3)$$

where k is the rate constant value for the metal biosorption determined by the most appropriate kinetic model (the pseudo-first-order or the pseudo-second-order kinetic model), Ea is the activation energy in kJ mol^{-1}, T is the temperature in Kelvin and R is the gas constant (8.314 J mol^{-1} K^{-1}).

The pseudo-first-order rate Lagergren model is [31–33]:

$$\frac{dq}{dt} = k_1(q_e - q_t) \quad (4)$$

where q_t and q_e (mg g^{-1}) are the amount of aluminum ions biosorbed at time t and at equilibrium respectively, k_1 (min^{-1}) is the rate constant of first-order adsorption. The integrated form of Eq. (4) is

$$\log(q_e - q_t) = \log q_e - \frac{k_1}{2.303} t \quad (5)$$

q_e and k_1 can be determined from the intercept and slope of the linear plot of $\log(q_e - q_t)$ versus t [25–34].

The pseudo-second-order kinetic model is expressed as [31–33]:

$$\frac{dq}{dt} = k_2(q_e - q_t) \quad (6)$$

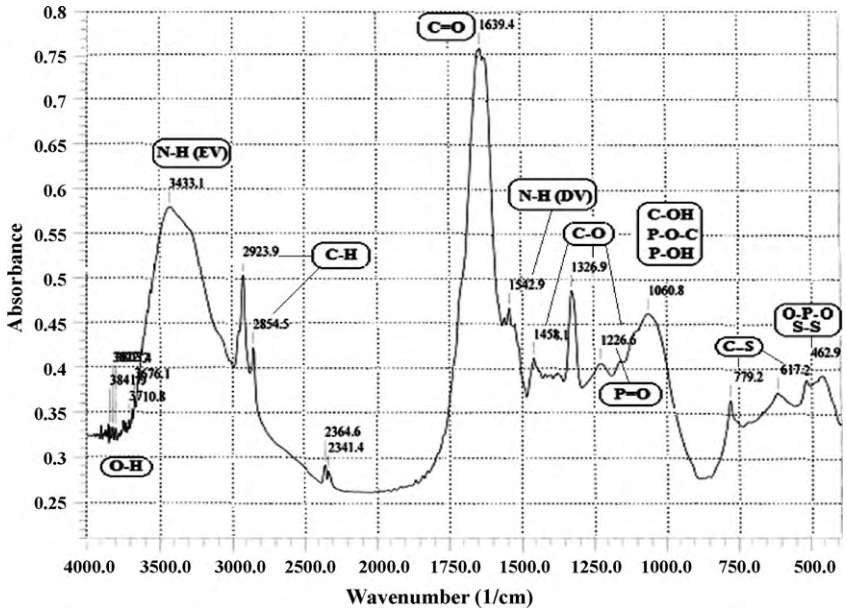

Fig. 1. Infrared spectrum of unloaded *S. rimosus* biomass. EV: Elongation vibration, DV: Deformation vibration.

where k_2 ($g\,mg^{-1}\,min^{-1}$) is the rate constant of second-order adsorption. Eq. (6) can be rearranged and linearized to obtain:

$$\frac{t}{q_t} = \frac{1}{k_2 q_e^2} + \frac{1}{q_e} t \quad (7)$$

The plot t/q_t versus t should give a straight line if second-order model is applicable and q_e and k_2 can be determined from the slope and intercept of the plot, respectively [25–34].

2.3.5. Effect of pH

The pH is an essential parameter in the biosorption process. It affects the metal solubility, its ionic form and the ionization of biosorbent groups. The effect of this parameter was studied under the following conditions: the particle size ranging from 250 μm to 560 μm, the biosorbent content $m = 25\,g\,L^{-1}$, the stirring speed $\omega = 250$ rpm, the temperature $T = 25\,^{\circ}C$, the initial concentration $C_0 = 30\,mg\,L^{-1}$, the solution volume was 250 mL, and pH_i was ranging from pH_i 2 to pH_i 4. In order to complete our study, we have studied the effect of two fixed pH: pH_f 3 and pH_f 4.

2.4. Biosorption isotherms

The biosorption isotherms were performed with variation of initial concentrations ranging from $30\,mg\,L^{-1}$ to $960\,mg\,L^{-1}$, under optimum conditions, at free pH (pH_i 4) and fixed pH (pH_f 4).

3. Results and discussion

3.1. Structural characterization by infrared spectroscopy analysis

The infrared spectroscopy analysis permitted to identify the characteristic bands of hydroxyl, methyl, carboxyl, amino, thiol and phosphate groups (Fig. 1). This result is in perfect conformity with the chemical composition of the wall and the cellular membrane of the used biosorbent. Indeed, *S. rimosus* wall is composed of peptidoglycan carrier of carboxyl, hydroxyl, amino and methyl functions; of teichoïc acids carriers of phosphate groups. Its cellular membrane is constituted of proteins which carry carboxyl, amino, hydroxyl, methyl and thiol functions and of phospholipids carriers of phosphate groups [35,36]. Similar results were reported by Selatnia et al. [21–24].

3.2. Aluminum biosorption kinetic

3.2.1. Effect of particle size

The size of adsorbent particles affects significantly the accumulation speed and the necessary time to achieve biosorption equilibrium. The kinetics of aluminum biosorption becomes faster with the reduction of particle diameter (Fig. 2). This is explained by the increase of the external surface (the grains size reduction implies an increase of the flux crossing the external layer) and by an easier accessibility of sites by a reduction of the superficial diffusion stage [17].

The aluminum fixation capacities obtained after 120 min are inversely proportional to the particle size (Fig. 2). However, the biosorption capacities at equilibrium have very near values for the different diameters (results not shown) indicating that the active sites were reached but with an intra-granular diffusion speed penalizing the big particles: The intra particle diffusion controls the kinetic of fixation but not the equilibrium of solute between the two phases [37]. As a conclusion, the diffusion constraints do not significantly affect the metallic cation fixation compared to the major limiting phenomenon which is the solid saturation. These results

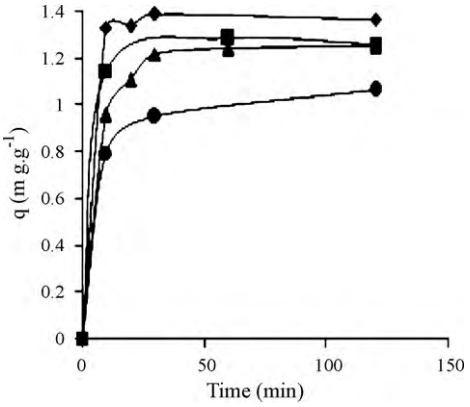

Fig. 2. Effect of particle size on the biosorption kinetic of aluminum onto *S. rimosus* biomass. ♦: ≤140 μm, ■:]140–250] μm, ▲:]250–560] μm, ●:]560–800] μm. $C_0 = 30\,mg\,L^{-1}$, $V = 250$ mL, pH_i 3.98, $\omega = 250$ rpm, $T = 25\,^{\circ}C$ and $m = 20\,g\,L^{-1}$.

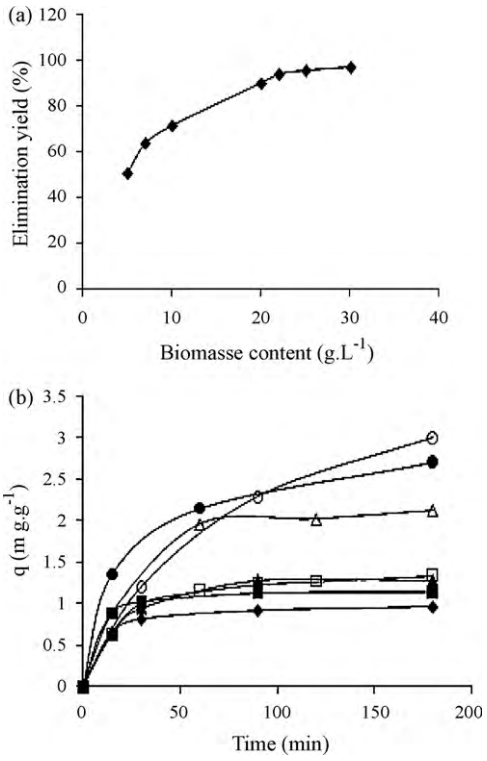

Fig. 3. Effect of biomass content on the aluminum biosorption onto *S. rimosus* biomass. a: Elimination yield obtained after 3 h of contact. b: Aluminum biosorption kinetic. ♦: 30 g L^{-1}, ■: 25 g L^{-1}, ▲: 22 g L^{-1}, □: 20 g L^{-1}, △: 10 g L^{-1}, ●: 7 g L^{-1}, ○: 5 g L^{-1}. The particle size:]250–560] μm, C_0 = 30 mg L^{-1}, V = 250 mL, pH$_i$ 3.98, ω = 250 rpm, T = 25°C.

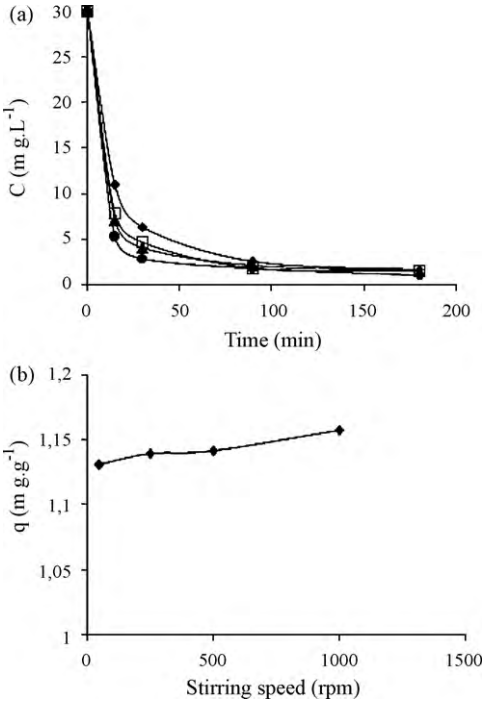

Fig. 4. Effect of agitation on the aluminum biosorption onto *S. rimosus* biomass. a: Aluminum biosorption kinetic. ♦: 50 rpm, □: 250 rpm, ▲: 500 rpm, ●: 1000 rpm. b: Biosorption capacities obtained after 3 h of contact. The particle size:]250–560] μm, C_0 = 30 mg L^{-1}, V = 250 mL, pH$_i$ 3.98, T = 25°C and m = 25 g L^{-1}.

are similar to those reported by Texier et al. [38] and Jansson-Charrier et al. [39].

The best kinetics of aluminum biosorption was observed for the three finer particle sizes. However, although it gave satisfactory results, the ranges: ≤140 μm and]140–250] μm present some inconveniences because they can cause some constraints in the industrial scale (ex: Clogging). The choice of]250–560] μm range is based on the fact that it presents a very close biosorption capacity to those of the two inferior ranges (q = 1.25 mg of Al(III) g^{-1} after 120 min) with a good mechanical behavior of the biosorbent (Fig. 2).

3.2.2. Effect of biosorbent content

The evolution of elimination yield (obtained after 180mn of contact) for different contents in biosorbent shows a dependent fixation on the quantity of this later, either an increase of the accumulation of the metallic cation with the introduced biosorbent mass (Fig. 3a). This is explained by the fact that the more the biosorbent content increases, the more the contact surface offered is important. A characteristic level appears, signifying that increasing the biosorbent mass would not increase the metal elimination rate (Fig. 3a). This is can be attributed to electrostatic interactions between the functional groups at the cell surfaces [40]. This saturation level that corresponds to the maximum rate of metallic cation elimination is obtained from a biomass content of 25 g L^{-1} for an initial concentration of 30 mg of Al(III) L^{-1}. Therefore, it is not useful, in practice, to increase the biosorbent content beyond these limits.

According to Marulanda and Harcum [41], the use of *Cyanidium caldarium* treated biomass at 5 g L^{-1} reveals a biosorption capacity of 1.4 mg of Al(III) g^{-1}. At the same conditions, the biosorption capacity obtained with *S. rimosus* is of 3 mg of Al(III) g^{-1} (Fig. 3b) with an elimination rate of 50.1% (Fig. 3a). Concerning the optimal content (25 g L^{-1}), the recorded capacity is 1.14 mg of Al(III) g^{-1} (Fig. 3b) with a best elimination rate of 95% (Fig. 3a).

3.2.3. Effect of agitation

The obtained results show that after 3 h of contact, the residual concentrations in Al(III) are very close for the different speeds of agitation (Fig. 4a). The agitation speed does not affect significantly the performance of aluminum biosorption phenomenon on *S. rimosus*. Indeed, agitation speed of 250 rpm allows a good homogenization, equilibrium establishment (Fig. 4a) and improves the biosorption capacity (Fig. 4b), contrary to the one of 50 rpm that reduces the solution homogeneity and forms a deposit of biosorbent grains, which delays the equilibrium establishment (Fig. 4a) [17,42]. Whereas, speeds of 500 rpm and 1000 rpm, present a slightly superior biosorption capacities (Fig. 4b) with the constraints related to the surplus of energy spent and to the biomass particle size modification (crumbling). The optimal speed of 250 rpm agrees with the one reported by Mameri et al. [17], Chergui et al. [19], Selatnia et al. [21–24] who noted a decline of the biosorption capacity beyond 250 rpm because of vortex phenomenon.

3.2.4. Effect of temperature (biosorption thermodynamics)

The temperature affects the kinetics of Al(III) fixation. In fact, the more the temperature increases, the more the necessary time to reach the equilibrium is reduced. This effect appears clearly when we pass from 10 °C to 25 °C and from 50 °C to 80 °C but not between 25 °C and 50 °C (Fig. 5). After 3 h of contact, the recorded biosorption capacities are close for all temperatures, except of the one of 10 °C. The temperature of 25 °C is then retained as an optimal temperature. Similar observations were described by Dilek et al. [42] and Strandberg et al. [43] who reported a positive effect of the temperature on the kinetics and the capacity of Uranium biosorption on *S. cerevisiae* (more important between 20 °C and 40 °C than between 40 °C and 50 °C) and the maximal capacity of Ni(II) ions fixation on

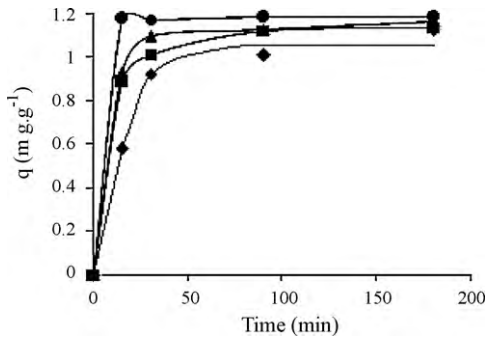

Fig. 5. Effect of temperature on the kinetic of aluminum biosorption onto *S. rimosus* biomass. ♦: 10 °C, ■: 25 °C, ▲: 50 °C, ●: 80 °C. The particle size:]250–560] μm, C_0 = 30 mg L^{-1}, V = 250 mL, pH_i 3.98, ω = 250 rpm, m = 25 g L^{-1}.

a fungic biomass (more marked from 20 °C to 25 °C than from 25 °C to 35 °C), respectively.

Some authors report that in the case of the endothermic biosorption, the increase of the temperature has a positive effect on the biosorption capacity [25,33,42–44]: the increase in biosorption with temperature may be attributed to either increase in the number of active surface sites available for biosorption on the adsorbent or the desolvation of the adsorbing species and the decrease in the thickness of the boundary layer surrounding the adsorbent with temperature, so that the mass transfer resistance of adsorbate in the boundary layer decreases. Since diffusion is an endothermic process, greater biosorption will be observed at higher temperature. Thus, the diffusion rate of ions in the external mass transport process increases with temperatures [33,45]. However, other authors noted a diminution of the biosorption yield with increasing temperature, suggesting a biosorption of exothermic nature [26–28].

In this work, with the exception of a slight improvement of the biosorption capacity between 10 °C and 25 °C, the effect of the temperature is particularly limited to the increase of metallic cation diffusion within the biosorbent since the equilibrium concentrations are close. Therefore, the biosorption of aluminum on *S. rimosus* seems to be of endothermic nature since the diminution of biosorption capacity with the increasing temperature was not observed (Fig. 5).

3.2.4.1. Evaluation of thermodynamic parameters (ΔG°, ΔH° and ΔS°). The ΔH° and ΔS° parameters were found to be 20.76 kJ mol^{-1} and 0.0685 kJ mol^{-1} K^{-1}, respectively (Fig. 6). The positive ΔH° indicates the endothermic nature of aluminum biosorption on *S. rimosus* biomass at 10–80 °C. Furthermore, the positive value of ΔS° reveals the increased randomness at the solid–solution interface during the fixation of the aluminum ions

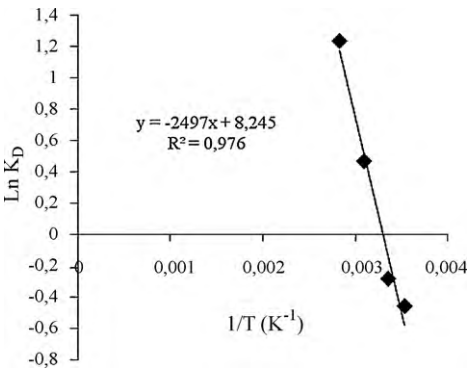

Fig. 6. Estimation of thermodynamic parameters for aluminum biosorption onto *S. rimosus* biomass: Plot of ln K_D versus $1/T$.

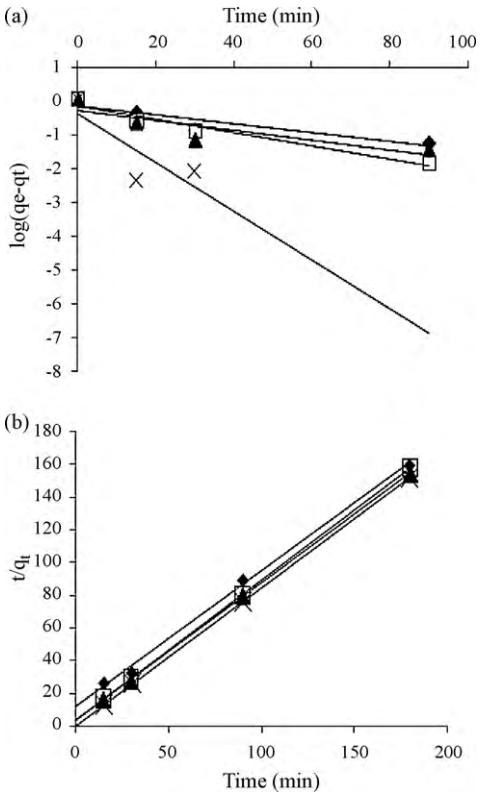

Fig. 7. Kinetic model plots at different temperatures. a: Pseudo-first-order model plot. b: Pseudo-second-order model plot. ♦: 10 °C, □: 25 °C, ▲: 50 °C, ×: 80 °C.

on the active sites of the biosorbent. ΔG° was calculated to be 1.07 kJ mol^{-1}, 0.69 kJ mol^{-1}, −1.26 kJ mol^{-1} and −3.62 kJ mol^{-1} at 10 °C, 25 °C, 50 °C and 80 °C, respectively. The negative ΔG° values (at 50 °C and 80 °C) indicate the thermodynamic feasibility and spontaneous nature of the biosorption. The increase in negative ΔG° values at 80 °C (in relation to 50 °C) shows an increase in biosorption feasibility at this temperature. At 10 °C, ΔG° is positive, reflecting a low diffusion speed of aluminum (Fig. 5). At 25 °C, the value of ΔG° is also positive but lower to the one recorded at 10 °C, indicating the feasibility improvement of the biosorption between 10 °C and 25 °C (Fig. 5).

The magnitude of ΔH° gives information on the type of biosorption, which can be either physical or chemical. The enthalpy or heat of biosorption, ranging from 0.5 kcal mol^{-1} to 5 kcal mol^{-1} (2.1–20.9 kJ mol^{-1}) corresponds a physical sorption as it ranges from 20.9 kJ mol^{-1} to 418.4 kJ mol^{-1} in case of a chemical sorption [30,34]. In our case, ΔH° is situated between the heat ranges of chemical and physical sorptions. Therefore, the biosorption of Al(III) on *S. rimosus* may be an intermediate process as an ionic exchange which is different of the physical biosorption (which requires a weak attractive force of type "wan der waals") and it does not require the establishment of strong chemical bonds.

3.2.4.2. Determination of activation energy. In order to calculate the activation energy of Al(III) ion sorption on *S. rimosus*, the values of the rate constants at different temperatures were determined with the pseudo-first-order and pseudo-second-order rate equations.

The first-order rate constant (k_1) and (q_e) values were determined from the intercept and slope of the linear plot of $\log(q_e - q_t)$ versus t (Fig. 7a). The pseudo-second-order biosorption rate constant (k_2) and (q_e) values were determined from the slope and intercept of the plots of t/q_t against time, t (Fig. 7b). The values of the rate constant and calculated q_e (for the two models) are presented in Table 1 along with the correlation coefficient.

Table 1
A comparison of the first-order and the second-order models at different temperatures (the particle size:]250–560] μm, C_0 = 30 mg L^{-1}, V = 250 mL, pH$_i$ 3.98, ω = 250 rpm, m = 25 g L^{-1}).

	$q_{e,exp}$ (mg g^{-1})	Pseudo-first-order kinetic model				Pseudo-second-order kinetic model			
		Equation	k_1 (min^{-1})	R^2	q_e (mg g^{-1})	Equation	k_2 (g mg^{-1} min^{-1})	R^2	q_e (mg g^{-1})
10 °C	1.07	$y = -0.009x - 0.131$	0.020727	0.81	0.73	$y = 0.827x + 11.51$	0.059420	0.99	1,20
25 °C	1.14	$y = -0.019x - 0.162$	0.043757	0.95	0.68	$y = 0.854x + 3.792$	0.192330	0.99	1.17
50 °C	1.17	$y = -0.014x - 0.297$	0.032242	0.74	0.5	$y = 0.838x + 3.090$	0.227263	0.99	1.19
80 °C	1.19	$y = -0.071x - 0.371$	0.163513	0.66	0.43	$y = 0.842x + 0.095$	7.462778	1.00	1.18

As can be seen from Table 1, the correlation coefficient for the pseudo-first-order kinetic model at the various temperatures was found to be situated between 0.66 and 0.95. Also, the equilibrium uptake (q_e) values calculated from the pseudo-first-order kinetic model did not agree well with the experimental ($q_{e,exp}$) values. It was also noticed that the correlation coefficient, R^2, for the pseudo-second-order rate equation was greater (0.99–1). Further, the theoretical equilibrium uptake (q_e) values agreed very well with the experimental ($q_{e,exp}$) data in the case of pseudo-second-order kinetic model. Hence, it was concluded that this sorption system was better described by second-order rate equation than by the first-order one. This conclusion is in agreement with literature [25–34].

Fig. 8 shows the corresponding linear plot of $\ln k_2$ against $1/T$ with a correlation coefficient of 0.85. The activation energy for aluminum biosorption on *S. rimosus* biomass was 52.18 kJ mol^{-1} derived from the slope of this plot.

The magnitude of activation energy may give an idea about the type of sorption. The activation energy for physical adsorption is usually no more than 4.2 kJ mol^{-1} (1.0 kcal mol^{-1}), since the forces involved in physical adsorption are weak. Chemical adsorption is specific and involves forces much stronger than in physical sorption. So the activation energy for chemical adsorption is of the same magnitude as the heat of chemical reactions. Two kinds of chemical adsorption are encountered, activated and, less frequently, non-activated. Activated chemical adsorption means that the rate varies with temperature according to a finite activation energy (between 8.4 kJ mol^{-1} and 83.7 kJ mol^{-1}) in the Arrhenius equation (high Ea). In non-activated chemical adsorption, chemisorption occurs very rapidly, suggesting the activation energy is near zero [46].

The aluminum biosorption process on *S. rimosus* is therefore an activated chemisorption. It requires a moderate energy (52.18 kJ mol^{-1}) and may involve a spontaneous sorption mechanism as an ion exchange where chemical bonds are not of strong energies (electrostatic bonds).

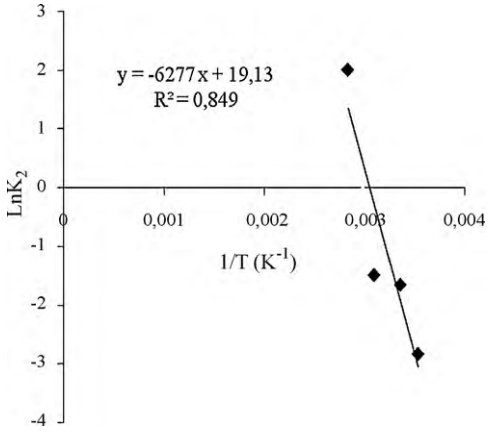

Fig. 8. Determination of activation energy for aluminum biosorption onto *S. rimosus* biomass: Plot of $\ln k_2$ versus $1/T$ for the estimation activation energy.

3.2.5. Effect of pH

In this part, we studied the effect of pH on the efficiency to bind Al(III) on *S. rimosus* biomass. The results, presented in Fig. 9a and b, indicate that at pH$_i$ 2 the efficiency of the biomass to remove Al(III) ions is practically negligible (0.002 mg g^{-1}). It was also observed at this condition that the pH, during the experiment, was slowly changing and did not exceed 2.5 (Fig. 9b). Two other pH (pH$_i$ 3, pH$_i$ 4) present faster biosorption kinetics, while final binding capacities, observed for both pH, are very close (1.11 mg g^{-1}). It is important to note that pHs measured at the end of the experiments are in the same range (pH ≈ 4).

These results could be explained by the competition between H$^+$ and Al(III) ions. The protons at higher concentration (pH 2) transform completely active sites as protonated form (COOH), resulting in a negligible ability of the biomass to bind aluminum ions. At higher pH (pH 3 and pH 4), a competition between H$^+$ and Al(III) is encountered: carboxylic sites begin to free their protons and to bind Al(III) cations. The number of anionic sites is than more important and biosorption capacity is improved. Aluminum biosorption was also tested at fixed pHs (Fig. 9a): pH$_f$ 3 (3–3.1) permits to have 38.68–44.26% (an average of 41.47%) of carboxyl groups in negative charge $\left(P\%_{COO^-} = 10^{pH-pK}/(1+10^{pH-pK})\right.$ and the average of pK$_{COOH}$ = 3.2), the biosorption capacity is 0.62 mg g^{-1} (51.83% of elimination yield). At pH$_f$ 4 (3.96–4.11), 85.19–89.04% (an average of 87.11%) of carboxyl groups are dissociated and are able to bind

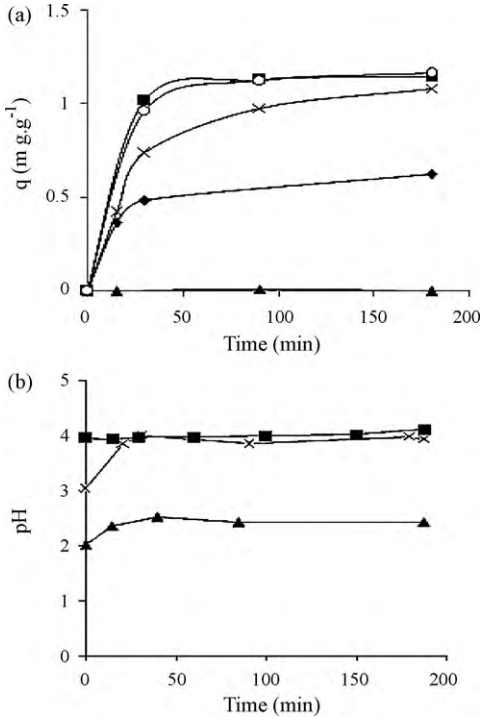

Fig. 9. a: Effect of pH on aluminum biosorption onto *S. rimosus* biomass. ▲: pH$_i$ 2, ×: pH$_i$ 3, ■: pH$_i$ 4, ♦: pH$_f$ 3, ○: pH$_f$ 4. b: Evolution of pH. The particle size:]250–560] μm, C_0 = 30 mg L^{-1}, V = 250 mL, ω = 250 rpm, m = 25 g L^{-1}.

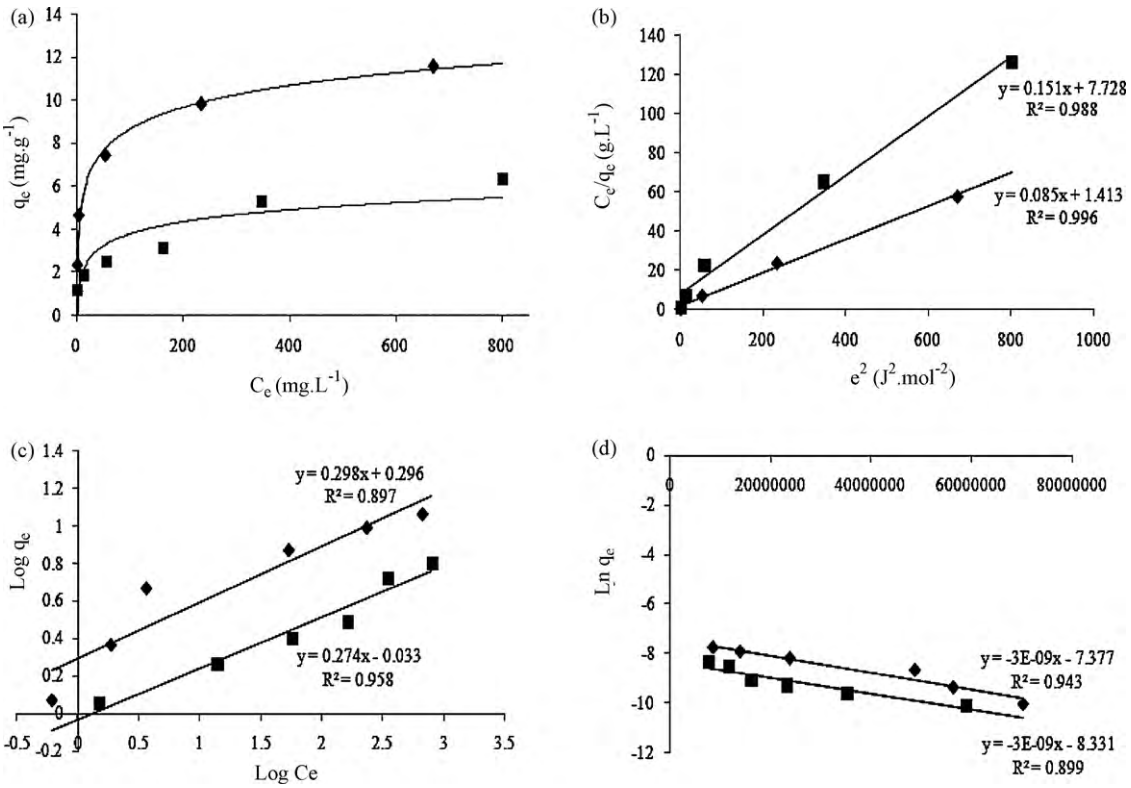

Fig. 10. Isotherms plots for aluminum biosorption onto *S. rimosus* biomass at free pH (pH_i 4) and fixed pH (pH_f 4). a: Plot of q_e versus C_e, b: Langmuir isotherm, c: Freundlich isotherm, d: D–R isotherm. ■: pH_i 4, ♦: pH_f 4, T = 25 °C, V = 250 mL, ω = 250 rpm, m = 25 g L^{-1}, C_0 = 30 mg L^{-1}, 60 mg L^{-1}, 120 mg L^{-1}, 240 mg L^{-1}, 480 mg L^{-1}, 960 mg L^{-1}.

metallic cations, this is the reason of the improvement of biosorption capacity (1.16 mg g^{-1} with elimination yield of 96.72%) and the rapid kinetic curves obtained at pH 4. The ratio between the obtained biosorption capacities at pH_f 3 and pH_f 4 is of 1.9. It is close to the one obtained for the dissociation percentages of COOH groups at the same pHs (1.9–2.3, an average of 2.1), which indicates that carboxyl groups give the main contribution in Al(III) biosorption. Moreover, it can be observed that at pH 2, carboxyl groups are mainly protonated (only 6% in negative form) but phosphoryl groups are deprotoned (pK_1 = 1.5, 76%). At this pH, the biosorption capacity is nil (0.002 mg g^{-1}), the contribution of phosphoryl groups in aluminum biosorption is then minimal.

Similar results were obtained by Jansson-Charrier et al. [39]: the biosorption capacity of Uranium on *Mucor miehei* is multiplied by 2 between pH 3 and pH 4. At week values of pH, protons exercise a competitive effect for biosorption sites. According to Sautel et al. [47], at pH 3 and pH 4 a competition between protons and Cd(II) ions during the biosorption experiments was encountered. The aluminum biosorption was not intensely studied since this metal presents a very narrow pH range permitting to bind metal without chemical precipitation. Marulanda and Harcum [41] found that the biosorption capacity of aluminum on *Cyanadium caldarium* increase with an increasing pH from pH 2 to pH 4. A maximum capacity was obtained at pH 5 without taking into account the chemical precipitation of aluminum ions at this pH. Sari and Tuzen [25] found that the biosorption efficiency of aluminum on *Padina pavonica* biomass was enhanced with pH increase; for further work, pH 4.5 was selected, at which the optimum recovery was achieved.

In practice, aluminum begins to precipitate between pH 4.5 and pH 5.0. The major functional groups (COOH) are ionized at pH greater than pH 3. A pH value fixed around 4 (4–4.25) is the optimum; it permits to have the soluble cationic form of aluminum and a maximum availability of anionic biosorption sites. Similar result was found by Al-Muhtaseb et al. [10].

3.3. Biosorption isotherms

To confirm the necessity to control the pH at 4, biosorption isotherms were achieved at fixed pH (pH_f 4) and free pH (pH_i 4). With free pH, a decrease of pH was observed: it is more pronounced with the concentration increase (results not shown). This result may be explained by the ion-exchange phenomenon between protons and Al(III), the amount of released H^+ is more important with the increase of concentration. The reduction of pH (from pHi 4 until an average of pH 3.24 at equilibrium) will reduce available functional groups sites able to fix the aluminum ions, biosorption capacities obtained at equilibrium are in the range of 1.14–6.34 mg g^{-1} (Fig. 10a). Thus, experiments with fixed pH_f 4 (4–4.25) were performed to use more efficiently Al(III) binding capacity of the biomass. Indeed, it was observed a significant improvement of binding capacity of biomass (biosorption capacities at equilibrium are in the range of 1.18–11.58 mg g^{-1}) (Fig. 10a). The comparison between free and controlled pH mode by means of biosorption isotherm curves indicates that biosorption phenomenon may be represented by isotherms of type I which represent a monolayer biosorption until the saturation of active sites (Fig. 10a). The biosorption isotherms were investigated using three equilibrium models, which are the Langmuir, Freundlich and Dubinin–Radushkevich (D–R) isotherm models [25–30,33,34] (Fig. 10b–d) (Table 2). The biosorption of aluminum onto *S. rimosus* biomass fitted well the Langmuir model (Fig. 10b). The correlation coefficients (R^2) were found to be 0.996 (for pH_f 4) and 0.988 (for pH_i 4). Calculated maximum capacities are close to maximum capacities obtained at equilibrium (Table 2, Fig. 10a): the effect of the pH on the performance of the biomass to bind Al(III) ions is clearly established since an increase of 6.6 mg g^{-1} (at free pH, pH_i 4) to 11.8 mg g^{-1} (at fixed pH, pH_f 4) was obtained. It can be noted that dissociation constant (K_d) decreases, therefore the affinity increases ($K_{L(pH_f\,4)} = 3K_{L(pH_i\,4)}$). The affinity expresses a degree

Table 2
Adsorption isotherms for aluminum biosorption on *S. rimosus* biomass: Equilibrium parameters (T = 25 °C, V = 250 mL, ω = 250 rpm, m = 25 g L^{-1}, C_0 = [30–960 mg L^{-1}]).

Langmuir isotherm $(C_e/q_e) = (1/K_L q_m) + (C_e/q_m)$			Freundlich isotherm $\log q_e = \log K_F + ((1/n)\log C_e)$			D–R isotherm $\ln q_e = \ln q_m - K_{DR}\varepsilon^2$ $\varepsilon = RT\ln(1 + (1/C_e))$		
	pH_f 4	pH_i 4		pH_f 4	pH_i 4		pH_f 4	pH_i 4
R^2	0.988	0.996	R^2	0.897	0.958	R^2	0.899	0.943
q_m (mg g^{-1})	11.76	6.62	K_F	1.98	0.93	q_m (mol g^{-1})	6.25×10^{-4}	2.41×10^{-4}
						q_m (mg g^{-1})	16.86	6.5
K_L (L mg^{-1})	0.060	0.0195	$1/n$	0.298	0.274	K_{DR} (mol^2 J^{-2})	3×10^{-9}	3×10^{-9}
$K_d = 1/K_L$ (mg L^{-1})	16.66	51.28	n	3.36	3.65	$E = (2K_{DR})^{-0.5}$ (kJ mol^{-1})	12.91	12.91

C_e: equilibrium concentration; q_e: adsorption capacity at equilibrium; q_m: maximum capacity; K_L: Langmuir constant (affinity); K_F: Freundlich constant; K_{DR}: the activity coefficient; and ε: the Polanyi potential.

of adsorbent–Al(III) interaction and its increase indicates the availability of more anionic sites (COO^-) to bind metallic cations at pH_f 4. It is interesting to notice that the ratio between the maximum binding capacities (at pH_i 4 and pH_f 4) is in the same range of the ratio obtained from the percentages of available carboxylic sites at pH_i 4 (52.46%) (the average of pH at equilibrium is pH 3.24) and pH_f 4 (4–4.25) (86.31–91.81%). Yang and Volesky [48] reported that biosorption of Uranium on a *Sargassum* biomass, showed a maximum binding capacity and an increase of affinity after variation of pH parameter from pH 3.2 to pH 4.

Freundlich and D–R isotherms are not as adequate as Langmuir model ($0.90 \leq R^2 \leq 0.96$) (Fig. 10c and d). The relationship between the amounts of sorbed aluminum and its equilibrium concentration in the solution is not adequately described. The maximum capacity (q_m) calculated by D–R isotherm at free pH (pH_i 4) is close to q_m obtained by Langmuir model (Table 2). At fixed pH (pH_f 4), q_m is more important, which confirm the increase of anionic sites at pH 4; but, it is not compatible with q_m obtained by Langmuir model and experimental q_m obtained at equilibrium (Table 2, Fig. 10a). For Freundlich model, we note an increase in K_F at fixed pH ($K_{F(pH_f\,4)} = 2K_{F(pH_i\,4)}$). The $1/n$ value was between 0 and 1 indicating that the biosorption of Al(III) using *S. rimosus* biomass was favorable at studied conditions (Table 2).

The D–R isotherm model determines also the nature of biosorption processes. The E (kJ mol^{-1}) value gives information about biosorption mechanism (physical or chemical). If it lies between 8 kJ mol^{-1} and 16 kJ mol^{-1}, the biosorption process takes place by chemical ion exchange and while $E < 8$ kJ mol^{-1}, the biosorption process proceeds physically [25–30,33,34]. The mean biosorption energy was calculated to be 12.91 kJ mol^{-1} for controlled and free pH (Table 2). These results suggest that the biosorption processes of Al(III) by *S. rimosus* biomass could taking place by chemical ion-exchange mechanism because the sorption energies lie within 8–16 kJ mol^{-1}.

4. Conclusion

This work targeted three objectives: biosorption kinetic, biosorption equilibrium and thermodynamic studies concerning aluminum fixation on *S. rimosus* biomass. The infrared characterization of this biosorbent revealed the presence of hydroxyl, methyl, carboxyl, amine, thiol and phosphate groups.

The study of biosorption kinetic parameters (particle size, biomass content, agitation, temperature and pH), permitted to establish the following optimum conditions: particle size,]250–560] μm, pH 4–4.25, biomass content of 25 g L^{-1}, agitation of 250 rpm and temperature of 25 °C.

Among the three tested models (Langmuir, Freundlich and Dubinin–Radushkevich models), the Langmuir model is the most appropriate to describe aluminum biosorption isotherm at free pH (pH_i 4) and at fixed pH (pH_f 4). With controlled pH, the number of fixation sites is more important, the maximum biosorption capacity is neatly enhanced from 6.62 mg g^{-1} at free pH (pH_i 4) to 11.76 mg g^{-1} at fixed pH (pH_f 4). The carboxyl functions are therefore mainly involved in aluminum fixation.

The thermodynamic parameters (ΔG°, ΔH° and ΔS°) showed the feasibility, the endothermic and the spontaneous nature of the biosorption at 10–80 °C. Kinetic evaluation of experimental data showed that the biosorption processes of Al(III) followed well pseudo-second-order kinetics. The activation energy of biosorption was determined as 52.18 kJ mol^{-1} showing that the biosorption process is an activated chemisorption. The biosorption energy calculated for optimum conditions by D–R isotherm model (12.91 kJ mol^{-1}) suggests that the biosorption of Al(III) by *S. rimosus* biomass could be taken place by chemical ion-exchange mechanism.

References

[1] C. Bismut, Clinical Toxicology, Medicine-science. Flammarion, Paris, 2000, pp. 555–559.
[2] J.L. Vignes, G. Andre, F. Kapala, Data on the Main Chemicals: Metals and Materials, Ed. N°7, Educational Resource Center of Chemistry – union of physicists – French Society of Chemistry, Paris, 1997, pp. 223–234.
[3] R. Lauwerys, Industrial Toxicology and Professional Poisoning, Masson, Paris, 1999, pp. 131–137.
[4] P. Chapuis, A. Favier, Trace Elements in Nutrition and in Th erapeutic, Med. Int., Paris, 1995, pp. 112–116.
[5] P. Galle, The toxicity of aluminum, Research 17 (1986) 766–775.
[6] P. Chapuis, Trace Elements in Medicine and Biology, Tec.Doc. Lavoisier, Paris, 1991, pp. 625–639.
[7] R.M. Garrunto, R. Yanagihara, D.C. Gajdusek, Models of environmentally induced neurological disease: epidemiology and etiology amyotrophic lateral sclerosis and parkinsonism-dementia in the Western Pacific, Environ. Geochem. Health 12 (1990) 137–151.
[8] M. Meinck, H. Stooff, H. Kohlschütter, The Industrial Wastewater, Ed. Tec. Doc (Masson and Cie), Paris, 1977, pp. 733–734.
[9] P.M. Choksi, V.Y. Joshi, Adsorption kinetic study for the removal of nickel (II) and aluminum (III) from an aqueous solution by natural adsorbents, Desalination 208 (2007) 216–231.
[10] S.A. Al-Muhtaseb, M.H. El-Naas, S. Abdallah, Removal of aluminum from aqueous solutions by adsorption on date-pit and BDH activated carbons, J. Hazard. Mater. 158 (2008) 300–307.
[11] M. Horsfall Jnr, A.I. Spiff, Equilibrium sorption study of Al^{3+}, Co^{2+} and Ag^{+} in aqueous solutions by fluted pumpkin (Telfairia Occidentalis HOOK f) waste biomass, Acta Chim. Slov. 52 (2005) 174–181.
[12] H.S. Lee, J.H. Suh, I.B. Kim, T. Yoon, Effect of aluminum in two-metal biosorption by an algal biosorbent, Miner. Eng. 17 (2004) 487–493.
[13] H.S. Lee, J.H. Suh, Interference of aluminum in heavy metal biosorption by a seaweed biosorbent, Korean J. Chem. Eng. 18 (2001) 692–697.
[14] J. Tomko, M. Bačkor, M. Štofko, Biosorption of heavy metals by dry fungi biomass, Acta Metal. Slov. 12 (2006) 447–451.
[15] J. Yang, Q. Wang, Q. Luo, Q. Wang, T. Wu, Biosorption behavior of heavy metals in bioleaching process of MSWI fly ash by *Aspergillus niger*, Biochem. Eng. J. 46 (2009) 294–299.
[16] M. Tuzen, M. Soylak, Biosorption of aluminum on *Pseudomonas aeruginosa* loaded on Chromosorb 106 prior to its graphite furnace atomic absorption spectrometric determination, J. Hazard. Mater. 154 (2008) 519–525.
[17] N. Mameri, N. Boudries, L. Addour, D. Belhocine, H. Lounici, H. Grib, A. Pauss, Batch zinc biosorption by a bacterial nonliving *Streptomyces rimosus*, Water Res. 33 (1999) 1345–1354.
[18] L. Addour, D. Belhocine, N. Boudries, Y. Comeau, A. Pauss, N. Mameri, Zinc uptake by *Streptomyces rimosus* biomass using a packed-bed column, J. Chem. Technol. Biotechnol. 74 (1999) 1089–1095.
[19] A. Chergui, M.Z. Bakhti, A. Chahboub, S. Haddoum, A. Selatnia, G.A. Junter, Simultaneous biosorption of Cu^{2+}, Zn^{2+} and Cr^{6+} from aque-

ous solution by *Streptomyces rimosus* biomass, Desalination 206 (2007) 179–184.
[20] I. Bakkaloglu, T.J. Butter, L.M. Evison, F.S. Holland, I.C. Hancock, Screening of various types biomass for removal and recovery of heavy metals (Zn, Cu, Ni) by biosorption, sedimentation and desorption, Water Sci. Technol. 38 (1998) 269–277.
[21] A. Selatnia, A. Boukazoula, N. Kechid, M.Z. Bakhti, A. Chergui, Y. Kerchich, Biosorption of lead (II) from aqueous solution by a bacterial dead *Streptomyces rimosus* biomass, Biochem. Eng. J. 19 (2004) 127–135.
[22] A. Selatnia, M.Z. Bakhti, A. Madani, L. Kertous, Y. Mansouri, Biosorption of Cd^{2+} from aqueous solution by a NaOH-treated bacterial dead *Streptomyces rimosus* biomass, Hydrometallurgy 75 (2004) 11–24.
[23] A. Selatnia, A. Madani, M.Z. Bakhti, L. Kertous, Y. Mansouri, R. Yous, Biosorption of Ni^{2+} from aqueous solution by a NaOH-treated bacterial dead *Streptomyces rimosus* biomass, Miner. Eng. 17 (2004) 903–911.
[24] A. Selatnia, A. Boukazoula, N. Kechid, M.Z. Bakhti, A. Chergui, Biosorption of Fe^{3+} from aqueous solution by a bacterial dead *Streptomyces rimosus* biomass, Process Biochem. 39 (2004) 1643–1651.
[25] A. Sari, M. Tuzen, Equilibrium, thermodynamic and kinetic studies on aluminum biosorption from aqueous solution by brown algae (*Padina pavonica*) biomass, J. Hazard. Mater. 171 (2009) 973–979.
[26] A. Sari, M. Tuzen, Removal of mercury (II) from aqueous solution using moss (*Drepanocladus revolvens*) biomass: equilibrium, thermodynamic and kinetic studies, J. Hazard. Mater. 171 (2009) 500–507.
[27] A. Sarı, M. Tuzen, Kinetic and equilibrium studies of biosorption of Pb(II) and Cd(II) from aqueous solution by macrofungus (*Amanita rubescens*) biomass, J. Hazard. Mater. 164 (2009) 1004–1011.
[28] A. Sarı, M. Tuzen, Biosorption of As(III) and As(V) from aqueous solution by macrofungus (*Inonotus hispidus*) biomass: equilibrium and kinetic studies, J. Hazard. Mater. 164 (2009) 1372–1378.
[29] M. Tuzen, A. Sari, D. Mendil, O.D. Uluozlu, M. Soylak, M. Dogan, Characterization of biosorption process of As(III) on green algae *Ulothrix cylindricum*, J. Hazard. Mater. 165 (2009) 566–572.
[30] A. Sari, M. Tuzen, Biosorption of total chromium from aqueous solution by red algae (*Ceramium virgatum*): equilibrium, kinetic and thermodynamic studies, J. Hazard. Mater. 160 (2008) 349–355.
[31] V. Padmavathy, Biosorption of nickel (II) ions by baker's yeast: kinetic, thermodynamic and desorption studies, Biores. Technol. 99 (2008) 3100–3109.
[32] Z. Aksu, Equilibrium and kinetic modelling of cadmium (II) biosorption by *C. vulgaris* in a batch system: effect of temperature, Sep. Purif. Technol. 21 (2001) 285–294.
[33] E. Malkoc, Ni(II) removal from aqueous solutions using cone biomass of *Thuja orientalis*, J. Hazard. Mater. B137 (2006) 899–908.
[34] A. Sari, D. Mendil, M. Tuzen, M. Soylak, Biosorption of palladium(II) from aqueous solution by moss (*Racomitrium lanuginosum*) biomass: equilibrium, kinetic and thermodynamic studies, J. Hazard. Mater. 162 (2009) 874–879.
[35] F.C. Neidhardt, J.L. Ingraham, M. Schaechter, Physiology of the Bacterial Cell: a Molecular Approach, Masson, Paris, 1994, pp. 14–18.
[36] R.H. Garrett, C.M. Grisham, Biochemistry, second ed., De Boeck University, Paris, 2000, pp. 245–283.
[37] N. Milande, J.C. Roux, E. Fourest, Use of filamentous fungi for the recovery of metals in industrial effluents, Recent Prog. Process. Eng. 7 (1993) 19–24.
[38] A.C. Texier, Y. Andres, C. Faur-Brasquet, P. Le Cloirec, Fixed-bed study for lanthanide (La, Eu, Yb) ions removal from aqueous solutions by immobilized *Pseudomonas aeruginosa*: experimental data and modelization, Chemosphere 47 (2002) 333–342.
[39] M. Jansson-Charrier, E. Guibal, R. Surjous, P. Le Cloirec, Removal of heavy metals by adsorption on materials of biological origin, Tech. Sci. Meth. 6 (1994) 321–326.
[40] S. Al-asheh, Z. Duvnjak, Adsorption of copper and chromium by *Aspergillus cabonarius*, Biotechnol. Prog. 11 (1995) 638–642.
[41] A.L.B. Marulanda, S.W. Harcum, Removal of copper and aluminum ions from solution by immobilized *Cyanidium caldarium*, Waste Manage. Environ. Restor. 22 (2000) 223–237.
[42] F.B. Dilek, A. Erbay, U. Yetis, Ni (II) biosorption by polyporous versicolor, Process Biochem. 37 (2002) 723–726.
[43] G.W. Strandberg, S.E. Shumate II, J.R. Parrott, Microbial cells as biosorbents for heavy metals: accumulation of uranium by *Saccharomyces cervisiae* and *Pseudomonas aeruginosa*, Appl. Environ. Microbiol. 41 (1981) 237–245.
[44] F. Banat, S. Al-Asheh, F. Mohai, Batch zinc removal from aqueous solution using dried animal bones, Sep. Purif. Technol. 21 (2000) 155–164.
[45] A.K. Meena, G.K. Mishra, P.K. Rai, C. Rajagopal, P.N. Nagar, Removal of heavy metal ions from aqueous solutions using carbon aerogel as an adsorbent, J. Hazard. Mater. 122 (2005) 161–170.
[46] Z. Aksu, Determination of the equilibrium, kinetic and thermodynamic parameters of the batch adsorption of nickel(II) ions onto *Chlorella vulgaris*, Process Biochem. 38 (2002) 89–99.
[47] G. Sautel, C. Roulph, P. Le Cloirec, Biofixation of cadmium by the bacteria *Pseudomonas putida*, Recent Prog. Process. Eng. 5 (1991) 203–208.
[48] J. Yang, B. Volesky, Biosorption and elution of uranium with seaweed biomass, Int. Biohydrometall. Symp. Proc. B (1999) 483–492.